Science Signaling
AAAS

Protein Kinase C {eta} Is Required for T Cell Activation and Homeostatic Proliferation

Guo Fu, Jianfang Hu, Nathalie Niederberger-Magnenat, Vasily Rybakin, Javier Casas, Pia P. Yachi, Stephanie Feldstein, Bo Ma, John A. H. Hoerter, Jeanette Ampudia, Stephanie Rigaud, Florence Lambolez, Amanda L. Gavin, Karsten Sauer, Hilde Cheroutre and Nicholas R. J. Gascoigne (6 December 2011)
Science Signaling **4** (202), ra84. [DOI: 10.1126/scisignal.2002058]

The following resources related to this article are available online at http://stke.sciencemag.org.
This information is current as of 15 December 2011.

Article Tools Visit the online version of this article to access the personalization and article tools:
http://stke.sciencemag.org/cgi/content/full/sigtrans;4/202/ra84

Supplemental Materials *"Supplementary Materials"*
http://stke.sciencemag.org/cgi/content/full/sigtrans;4/202/ra84/DC1

References This article cites 41 articles, 19 of which can be accessed for free:
http://stke.sciencemag.org/cgi/content/full/sigtrans;4/202/ra84#otherarticles

Glossary Look up definitions for abbreviations and terms found in this article:
http://stke.sciencemag.org/glossary/

Permissions Obtain information about reproducing this article:
http://www.sciencemag.org/about/permissions.dtl

Downloaded from stke.sciencemag.org on December 15, 2011

Science Signaling (ISSN 1937-9145) is published weekly, except the last week in December, by the American Association for the Advancement of Science, 1200 New York Avenue, NW, Washington, DC 20005. Copyright 2008 by the American Association for the Advancement of Science; all rights reserved.

IMMUNOLOGY

Protein Kinase C η Is Required for T Cell Activation and Homeostatic Proliferation

Guo Fu,[1]* Jianfang Hu,[1†] Nathalie Niederberger-Magnenat,[1,2†‡] Vasily Rybakin,[1] Javier Casas,[1] Pia P. Yachi,[1§] Stephanie Feldstein,[1||] Bo Ma,[3§] John A. H. Hoerter,[1] Jeanette Ampudia,[1] Stephanie Rigaud,[1] Florence Lambolez,[2] Amanda L. Gavin,[1¶] Karsten Sauer,[1] Hilde Cheroutre,[2] Nicholas R. J. Gascoigne[1]*

Protein kinase C η (PKCη) is abundant in T cells and is recruited to the immunological synapse that is formed between a T cell and an antigen-presenting cell; however, its function in T cells is unknown. We showed that PKCη was required for the activation of mature CD8⁺ T cells through the T cell receptor. Compared with wild-type T cells, PKCη$^{-/-}$ T cells showed poor proliferation in response to antigen stimulation, a trait shared with T cells deficient in PKCθ, which is the most abundant PKC isoform in T cells and was thought to be the only PKC isoform with a specific role in T cell activation. In contrast, only PKCη-deficient T cells showed defective homeostatic proliferation, which requires self-antigen recognition. PKCη was dispensable for thymocyte development; however, thymocytes from mice doubly deficient in PKCη and PKCθ exhibited poor development, indicating some redundancy between the PKC isoforms. Deficiency in PKCη or PKCθ had opposing effects on the relative numbers of CD4⁺ and CD8⁺ T cells. PKCη$^{-/-}$ mice had a higher ratio of CD4⁺ to CD8⁺ T cells compared to that of wild-type mice, whereas PKCθ$^{-/-}$ mice had a lower ratio. Mice deficient in both isoforms exhibited normal cell ratios. Together, these data suggest that PKCη shares some redundant roles with PKCθ in T cell biology and also performs nonredundant functions that are required for T cell homeostasis and activation.

INTRODUCTION

The protein kinase C (PKC) family of serine and threonine kinases includes 10 isoforms in human and mouse, which play important roles in signal transduction in different cellular systems, including regulating differentiation, cell motility, secretion, growth, and death (*1*). Of the PKC isoforms found in T cells (α, δ, ε, η, and θ), only PKCθ is thought to have an important and specific role in T cell biology, where it is involved in costimulation of signal transduction in response to antigen recognition, leading to activation of transcription factors, including nuclear factor κB (NF-κB), and to changes in gene transcription, which results in responses such as increased secretion of the cytokine interleukin-2 (IL-2) (*2–5*). However, expression of the gene *Prkch*, which encodes PKCη, is increased during positive selection (*6*, *7*), and gene expression profiling has shown that *Prkch* mRNA abundance, like that of PKCθ, is higher in T cells than in other mouse or human cell types and organs (http://biogps.org/#goto=genereport&id=18755; gnf1m00727_at and U133A 206099_at), which suggests that PKCη may play a role in T cell biology. Although a PKCη-deficient mouse exists, no immunological studies of these mice have been reported (*8*).

PKCθ is recruited to the immunological synapse, the area of contact that is formed between mature T cells and antigen-presenting cells (APCs), where it concentrates in the central region (*9–11*). In addition, PKCθ associates with the co-receptor CD28 in microclusters that contain the T cell antigen receptor (TCR), which move centripetally into the immunological synapse and are thought to be important in the costimulation of T cells (*12*). A fusion protein of PKCη and green fluorescent protein (GFP) is also recruited to the immunological synapse upon TCR stimulation, where it is localized diffusely over the whole region (*13*). Studies with PKCθ$^{-/-}$ mice revealed the involvement of PKCθ in multiple signaling pathways downstream of TCR stimulation (*14–20*). Given the importance of PKCθ in mature T cells, it was surprising that initial studies showed no defect in T cell development in PKCθ$^{-/-}$ mice (*14*, *16*); however, another study found that PKCθ is indeed involved in thymocyte development, with PKCθ$^{-/-}$ mice showing a mild defect in positive selection (*21*). Redundancy between different PKC isoforms may obscure the importance of any individual PKC in T cell development and function in vivo.

Here, we confirmed that the abundance of PKCη mRNA is increased during the positive selection of thymocytes, and we found that PKCη, similar to PKCθ, was recruited to the immunological synapse. To further investigate the specific role of PKCη and the potential redundancy between PKCη and PKCθ in T cell development and mature T cell function, we generated mice deficient in *Prkch*, the gene encoding PKCη (PKCη$^{-/-}$ mice), and mice doubly deficient in *Prkch* and *Prkcq*, which encodes PKCθ, to generate PKCη$^{-/-}$PKCθ$^{-/-}$ double-knockout (DKO) mice. We found that although PKCη shared redundant functions with PKCθ during T cell development, PKCη was required for normal functions of mature T cells, because PKCη$^{-/-}$ T cells were less well able to proliferate in response to antigen or to undergo homeostatic proliferation than were wild-type mice, which was likely a result of impaired intracellular calcium

[1]Department of Immunology and Microbial Science, The Scripps Research Institute, 10550 North Torrey Pines Road, La Jolla, CA 92037, USA. [2]Department of Developmental Immunology, La Jolla Institute for Allergy and Immunology, 9420 Athena Circle, La Jolla, CA 92037, USA. [3]Department of Molecular and Experimental Medicine, The Scripps Research Institute, La Jolla, CA 92037, USA.
*To whom correspondence should be addressed. E-mail: gascoigne@scripps.edu (N.R.J.G.); guofu@scripps.edu (G.F.)
†These authors contributed equally to this work.
‡Present address: Faculty of Biology and Medicine, University of Lausanne, CH-1011 Lausanne, Switzerland.
§Present address: Applied Molecular Evolution, 3520 Dunhill Street, San Diego, CA 92121, USA.
||Present address: School of Medicine, University of California San Diego, 9500 Gilman Drive, La Jolla, CA 92093, USA.
¶Present address: Burnet Institute, 85 Commercial Road, Melbourne, Victoria 3004, Australia.

Downloaded from stke.sciencemag.org on December 15, 2011

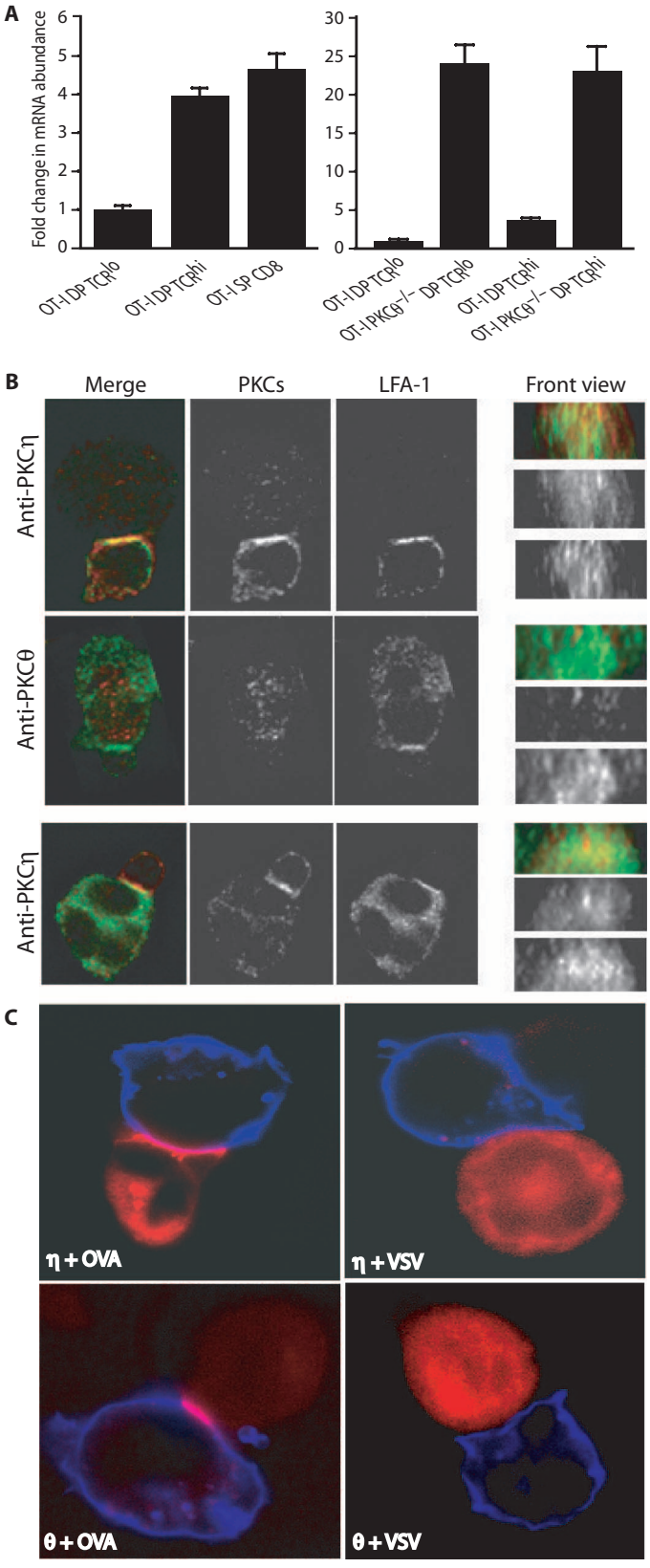

Fig. 1. Analysis of PKCη abundance and localization. (**A**) PKCη mRNA is increased in abundance during positive selection. PKCη mRNA abundance was determined by real-time RT-PCR. Results are shown as fold change compared to the amount of PKCη mRNA in OT-I DP TCR^{lo} cells. Data represent two experiments, each performed in duplicate. (**B**) PKCη recruitment to the immunological synapse in the absence of PKCθ. To avoid potential cross-reactivity of PKC-specific antibodies, we used thymocytes and mature T cells from PKCθ$^{-/-}$ mice. After activation with superantigen-loaded LK35 cells, T cells or thymocytes were incubated with antibodies against LFA-1 and the PKC isoforms (anti-PKCθ and anti-PKCη), after which they were incubated with antisera against rabbit immunoglobulin (Ig). In the merged image panel, LFA-1 staining is shown in green, whereas PKC staining is in red. The larger cells are LK35 cells and the smaller cells are T cells. Top and middle panels show thymocytes, and the bottom panels show mature T cells, with corresponding en face views shown on the right. Data represent at least 50 cell-cell conjugates of each type. (**C**) Recruitment of PKCη to the immunological synapse in live cells. OT-I T hybridomas transfected with plasmid encoding PKCη-RFP (η) or PKCθ-RFP (θ) were stimulated with EL4 cells that were pulsed with OVA or VSV peptides. PKC protein is shown in red, whereas EL4 cells are shown in blue. Images are representative of at least 20 cells collected from three experiments.

(Ca^{2+}) signaling and nuclear translocation of the transcription factor NF-κB, defects similar to those found in PKCθ$^{-/-}$ mice. In contrast to PKCη$^{-/-}$ and PKCθ$^{-/-}$ mice, DKO mice had a more severe defect in T cell development and more profound functional defects in mature T cells, as was revealed in multiple assays. Together, our data suggest that in addition to sharing redundant roles with PKCθ, PKCη has its own specific functions in T cell biology.

RESULTS

The abundance of PKCη mRNA is increased during positive selection of thymocytes

In a previous study, we showed that the abundance of *Prkch* mRNA (hereafter referred to as PKCη mRNA) is increased in preselection thymocytes when stimulated with an antibody against the Vβ chain of the TCR (*7*). Independently, Hogquist and colleagues also found that PKCη mRNA abundance is increased during positive selection (*6*). Given the requirement for PKCθ for antigenic stimulation in mature T cells (*9*, *10*, *14*, *16*), it was surprising that PKCη rather than *Prkcq* mRNA (hereafter referred to as PKCθ mRNA) abundance was increased during positive selection (*7*). To investigate whether PKCη was involved in thymocyte positive selection in vivo and to test whether PKCη might compensate for the loss of PKCθ, we measured PKCη mRNA amounts by real-time reverse transcription–polymerase chain reaction (RT-PCR) assay. We found that PKCη mRNA was increased in abundance in late-stage CD4^{+} and CD8^{+} double-positive (DP) cells and in CD4^{+} single-positive (SP) and CD8^{+} SP cells, that is, in cells that had undergone positive selection (Fig. 1A, left). DP cells with a high abundance of TCR as assessed by flow cytometry (TCR^{hi} DP cells) showed about a fourfold increase in PKCη mRNA abundance compared to that in TCR^{lo} DPs, and this abundance remained increased in the SP cells. Because PKCθ is found in earlier developmental stages in thymocytes than is PKCη, if there was redundancy between the PKCθ and the PKCη isoforms, we would expect that PKCη would be produced earlier in cells in the absence of PKCθ. Indeed, we found that expression of the gene

Downloaded from stke.sciencemag.org on December 15, 2011

encoding PKCη was induced earlier and to a greater extent than normal in cells before positive selection (TCR^{lo} DP cells) (Fig. 1A, right). These results suggested that PKCη might play a role in thymocyte development.

PKCη is recruited to the immunological synapse

Because the gene encoding PKCη was induced during normal positive selection and because it was expressed earlier and to a greater extent in $PKC\theta^{-/-}$ thymocytes than in wild-type thymocytes, we tested whether PKCη, like PKCθ, was recruited to the immunological synapse in thymocytes. The recruitment of PKCθ to the synapse is important in signal transduction and is a hallmark of the recognition by the T cell of antigenic peptide presented by major histocompatibility complex (MHC). To avoid the possibility of cross-reaction between antibodies against PKCη and PKCθ, we first isolated thymocytes and mature T cells from $PKC\theta^{-/-}$ mice and activated them with APCs that presented the superantigens staphylococcal enterotoxin A (SEA) and SEB, which react with more than 40% of the Vβ repertoire of TCRs in B6 mice (*22*). Superantigens like SEA and SEB bind to MHC class II molecules and are then able to activate T cells by binding to the TCR through recognition of Vβ sequences. PKCη was recruited to the immunological synapse in thymocytes and in mature T cells upon stimulation with SEA and SEB (Fig. 1B). In PKCθ-sufficient thymocytes, PKCθ, but not PKCη, was present at the immunological synapse of DP cells before selection (PKCη is not yet present in these cells) (fig. S1). In SP cells, both PKCθ and PKCη were found at the immunological synapse. In $PKC\theta^{-/-}$ thymocytes, PKCη mRNA was detected in less mature DP cells than in wild-type thymus (Fig. 1A), and, consequently, PKCη was present in the immunological synapses of DP cells (fig. S2).

To visualize the recruitment of PKCη to the immunological synapse in live cells, we transfected OT-I hybridoma cells (*23*), which have a TCR that recognizes a peptide from ovalbumin (OVA) presented on the MHC class I molecule $H2\text{-}K^b$, with plasmids encoding mouse PKCη fused to red fluorescent protein (PKCη-RFP) or PKCθ-RFP. We stimulated these cells with EL4 cells that had been incubated ("pulsed") with different peptides. When the stimulatory OVA peptide was presented to the OT-I cells, both PKCη and PKCθ were recruited to the immunological synapse; however, when the nonstimulatory vesicular stomatitis virus (VSV) peptide was presented, no such recruitment took place, which demonstrated that the recruitment of PKCη to the immunological synapse was antigen-specific (Fig. 1C). Jurkat cells, a human $CD4^+$ T cell line, were transfected with plasmids encoding GFP-tagged human PKCη, PKCθ, and PKCα proteins (fig. S3A). PKCη and PKCθ, but not PKCα, were recruited to the immunological synapse during recognition of a superantigen ligand. Similarly, stimulation of an MHC class II–restricted T cell hybridoma with antigenic peptide–pulsed APCs resulted in the concentration of transgenic fluorescence-tagged PKCη and PKCθ, but not PKCδ, at the immunological synapse (fig. S3B). To compare the recruitment of PKCη and PKCθ directly, we cotransfected OT-I cells with plasmids encoding PKCη-RFP and PKCθ-GFP and imaged the fluorescent proteins during antigen recognition (fig. S4). Both PKCη and PKCθ were recruited to the immunological synapse; however, whereas PKCη remained in a diffuse pattern over the whole area of the synapse (Fig. 1, B and C), which was consistent with an earlier study (*13*), PKCθ was more centrally concentrated at the immunological synapse (Fig. 1, B and C), as was expected from previous work (*9*, *10*).

PKCη is not required for positive or negative selection of thymocytes

To investigate the role of PKCη in a broader manner, we generated *Prkch*-deficient ($PKC\eta^{-/-}$) mice (fig. S5). The thymi of $PKC\eta^{-/-}$ mice contained ~20% fewer cells than did the thymi of wild-type mice. When we analyzed thymocyte subsets in the thymi of $PKC\eta^{-/-}$ mice, we found that the numbers of double-negative 1 (DN1) and DN4 cells were reduced compared to those in thymi from wild-type mice; however, the numbers of DN2 and DN3 cells were not altered (Fig. 2A). DN4 cells develop into $CD4^+CD8^+$ DP cells, after which they are subjected to positive and negative selection to generate self-MHC–restricted, self-antigen–tolerant mature T cells (*24*). The proportions of DP, $CD4^+$ SP, and $CD8^+$ SP subsets were similar in the thymi of $PKC\eta^{-/-}$ and wild-type mice, with slightly reduced cell numbers of DP subsets in the $PKC\eta^{-/-}$ mice (Fig. 2B). These results suggested that PKCη was not required for the positive selection of thymocytes.

To investigate the role of PKCη in negative selection, we used a superantigen-mediated deletion model. Mouse mammary tumor proviruses (Mtv) encode superantigens that are presented by the MHC class II molecule I-E to T cells, resulting in the intrathymic deletion of cells bearing

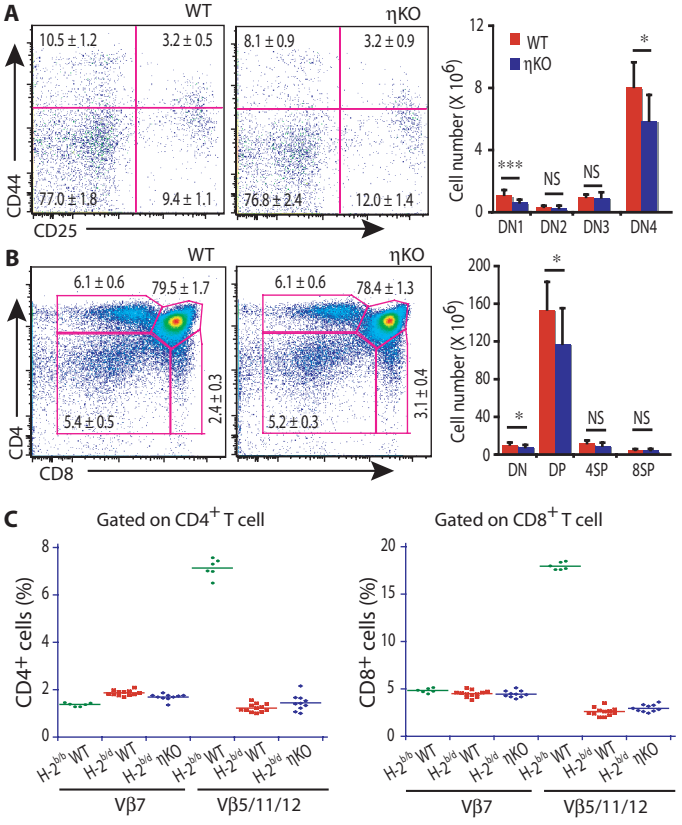

Fig. 2. Thymocyte development in $PKC\eta^{-/-}$ mice is normal. (**A** and **B**) Thymocytes from age- and sex-matched wild-type (WT) (n = 8 mice) and $PKC\eta^{-/-}$ mice (ηKO, n = 8 mice) were analyzed for the presence of (A) $CD4^-CD8^-$ (DN) subsets and (B) $CD4^+$ and $CD8^+$ (DP, SP) and DN subsets. Left: representative flow cytometry plots showing the mean percentages of each subset ± SD. Right: mean total numbers of cells ± SD for each subset. P values were calculated by Student's t test. $^*P \leq 0.05$; $^{***}P \leq 0.001$. NS, not significant. (**C**) Negative selection of $PKC\eta^{-/-}$ thymocytes is normal. T cells expressing Vβ5, Vβ11, or Vβ12, but not Vβ7, were deleted by endogenous mouse mammary tumor virus–encoded superantigens in mice that express I-E ($H\text{-}2^{b/d}$) but not in mice lacking I-E ($H\text{-}2^{b/b}$). $PKC\eta^{-/-}$ thymocytes bearing Vβ5, Vβ11, or Vβ12 were deleted similarly to wild-type thymocytes. Each dot represents a single mouse.

Downloaded from stke.sciencemag.org on December 15, 2011

Vβ elements recognized by particular Mtv superantigens (*22*, *25*). Because B6 (MHC haplotype H-2^b) mice do not express I-E, we crossed the B6 PKCη$^{-/-}$ mice to B10.D2 (H-2^d) mice, producing F1 H-$2^{b/d}$ mice that express I-E^d. In combination with the endogenous superantigens Mtv-8 and Mtv-9, which are carried by both B6 and B10.D2 cells, I-E causes the deletion of thymocytes that express the Vβ5, Vβ11, and Vβ12 chains of the TCR on their surface (*22*, *25*). When we compared H-$2^{b/b}$ mice with H-$2^{b/d}$ PKCη$^{+/+}$ mice, we found that a substantial number of T cells expressing Vβ5, Vβ11, and Vβ12 TCRs were deleted in the H-$2^{b/d}$, I-E–expressing F1 mice (Fig. 2C). Vβ7$^+$ T cells do not recognize Mtv-8 and Mtv-9 superantigens and thus were not deleted in either mouse. Superantigen-mediated negative selection was as efficient in the H-$2^{b/d}$ PKCη$^{-/-}$ as in PKCη$^{+/+}$ mice, indicating that PKCη was dispensable for superantigen-mediated negative selection.

PKCη-deficient mice have increased numbers of T cells with a memory phenotype

We observed that the lymph nodes of PKCη$^{-/-}$ mice were larger than those of wild-type mice (Fig. 3A). In the cervical area, there were more and larger readily identifiable lymph nodes in PKCη$^{-/-}$ mice than in wild-type mice (Fig. 3A, left). When we isolated the axillar, brachial, and inguinal lymph nodes, we found that they were larger in PKCη$^{-/-}$ mice than in wild-type mice (Fig. 3A, right). Consistent with this finding, the number of lymph node cells was increased in the PKCη$^{-/-}$ mice compared to that in the wild-type mice (Fig. 3B). These data suggested that PKCη$^{-/-}$ mice may have a general overproduction of lymphocytes rather than swollen lymph nodes (lymphadenopathy); however, the number of lymphocytes in the spleens of PKCη$^{-/-}$ mice was less than that of wild-type mice (Fig. 3B). In the lymph nodes, although there were only minor changes in the proportions of T cells or B cells or in the T cell subpopulations [CD8$^+$, CD4$^+$CD25$^-$ conventional CD4$^+$ cells, or CD4$^+$CD25$^+$ regulatory T cells (T_{regs})] (Fig. 3C), the absolute number of each cell type was substantially increased in the PKCη$^{-/-}$ mice compared to those in

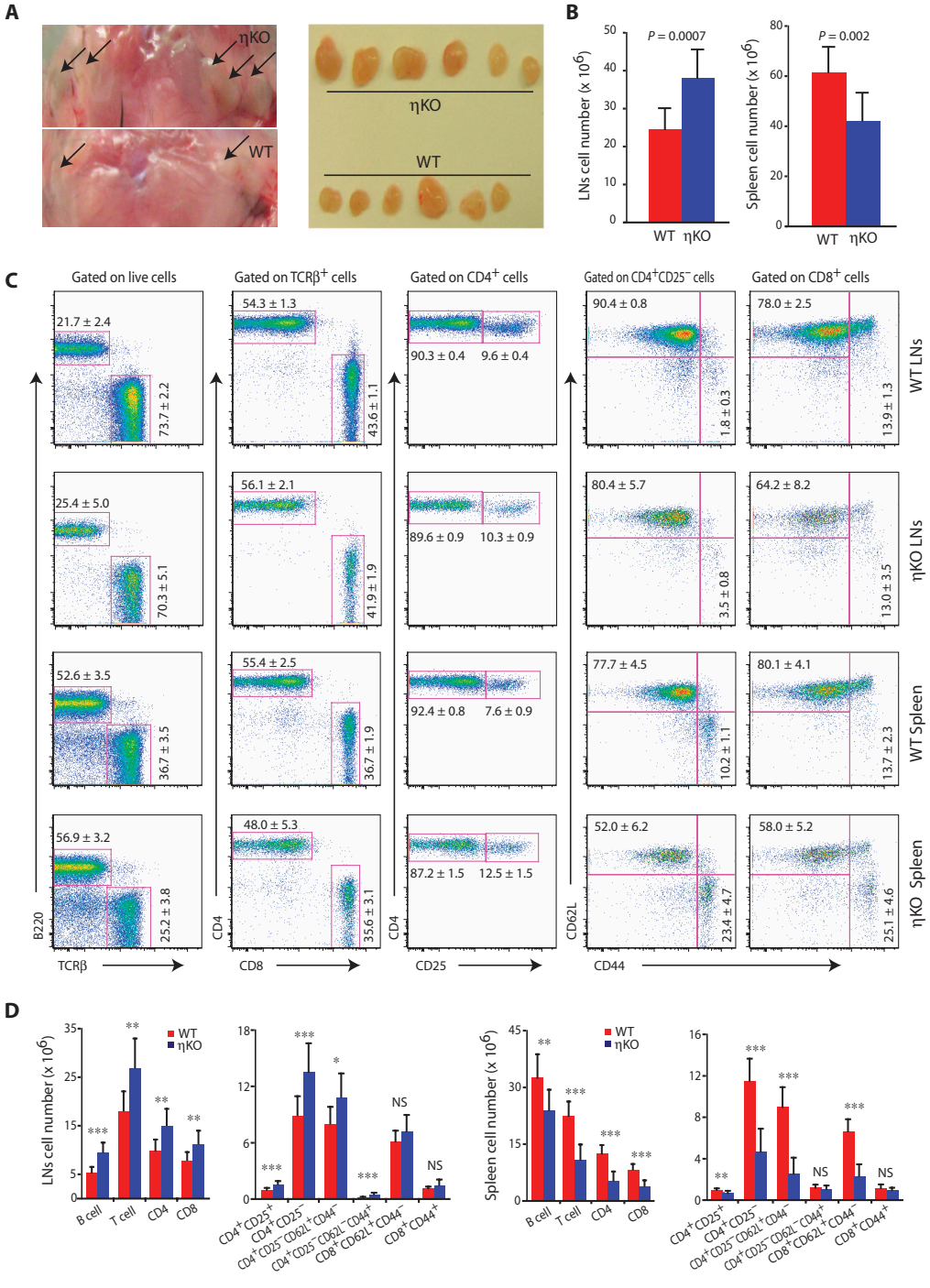

Fig. 3. PKCη$^{-/-}$ mice have enlarged lymph nodes. The mice analyzed in Fig. 2 were examined to determine the phenotype of their peripheral T cells. (**A**) Lymph nodes from the cervical area were photographed and are shown on the left; arrows indicate readily identifiable lymph nodes. On the right are axillar, brachial, and inguinal lymph nodes that were isolated from mice and aligned for comparison. (**B**) Total lymphocyte numbers from six pooled axillar, brachial, and inguinal lymph nodes are shown on the left, whereas total lymphocyte numbers from spleens are shown on the right. (**C**) Representative flow cytometry plots of lymph nodes (LNs) and spleens are shown with the proportion of each cell type listed as the mean ± SD. (**D**) Absolute cell numbers of the indicated subsets are listed for lymph nodes and spleen. For cell numbers, *P* values calculated by Student's *t* test are shown: **P* ≤ 0.05; ***P* ≤ 0.01; ****P* ≤ 0.001; NS, not significant; *n* = 8 mice. Data represent three experiments.

Downloaded from stke.sciencemag.org on December 15, 2011

wild-type mice (Fig. 3D), whereas the numbers of each cell type were lower in the spleens of PKCη$^{-/-}$ mice than in those of wild-type mice. The proportion of cells with a memory or activated phenotype within the conventional CD4$^+$CD25$^-$ population (CD44$^+$) of cells was increased in the lymph nodes and spleens of PKCη$^{-/-}$ mice compared to those in wild-type mice (Fig. 3, C and D). We obtained similar results when we used the transcription factor Foxp3, rather than the surface marker CD25, to define T_{regs} (fig. S6, A and B). The total numbers of lymph node and splenic lymphocyte subsets were similar in wild-type and PKCη$^{-/-}$ mice, which suggested that the lymphocytes of PKCη-deficient mice might preferentially home (or traffic) to the lymph nodes rather than to the spleen. The exception to this conservation in total lymphocyte number in the secondary lymphoid tissues was the decrease in the total number of naïve CD4$^+$CD25$^-$ and the increase in the number of CD4$^+$CD25$^-$ memory phenotype T cells in the PKCη$^{-/-}$ mice compared to those of wild-type mice, which suggested that the knockout cells may have responded to more self-stimulation in the periphery than did the wild-type cells (*26*).

PKCη-deficient T cells show impaired proliferation

To test the proliferative response of PKCη$^{-/-}$ T cells, we purified naïve CD4$^+$ or CD8$^+$ T cells from lymph nodes, stimulated them through the TCR with various concentrations of antibody against CD3, and measured their proliferative responses. Naïve CD4$^+$ and CD8$^+$ T cells from PKCη$^{-/-}$ mice proliferated less well than did naïve CD4$^+$ and CD8$^+$ T cells from wild-type mice (Fig. 4A). Unlike PKCθ$^{-/-}$ CD8$^+$ T cells whose proliferation was completely abrogated by loss of PKCθ, the proliferation of PKCη$^{-/-}$ CD8$^+$ T cells was only moderately reduced by 30 to 50% (Fig. 4A). So that both cell types could experience an identical cytokine environment, we determined cell division by measuring the dilution of the cytoplasmic dye carboxyfluorescein succinimidyl ester (CFSE) with a mixture of PKCη$^{-/-}$ T cells (which had the surface marker CD45.2) and PKCη$^{+/+}$ T cells (which had the surface marker CD45.1). CD8$^+$ T cells from PKCη$^{-/-}$ mice proliferated less well than did PKCη$^{+/+}$ cells in response to stimulation by antibody against CD3 or by cross-linking of T cell surface glycoproteins with the lectin concanavalin A (ConA) (Fig. 4B). We then performed a similar experiment with MHC class I–restricted OT-I TCR transgenic T cells that responded to different concentrations of OVA peptide presented by splenic APCs. In these experiments, PKCη$^{-/-}$ or PKCθ$^{-/-}$ T cells (which had the surface marker Thy1.2) were mixed with PKCη$^{+/+}$ T cells (which had the surface marker Thy1.1). The PKCη$^{-/-}$ T cells proliferated more weakly than did the PKCη$^{+/+}$ cells, but more strongly than did the PKCθ$^{-/-}$ cells (Fig. 4C).

To investigate the proliferation of PKCη$^{-/-}$ T cells under more physiological conditions, we stimulated OT-I TCR transgenic PKCη$^{-/-}$ T cells in vivo with bone marrow–derived dendritic cells (BMDCs) that were loaded with OVA peptide. We purified wild-type (Thy1.2$^+$CD45.2$^+$) and PKCη$^{-/-}$ (Thy1.1$^+$/Thy1.2$^+$CD45.2$^+$) OT-I T cells from lymph nodes, mixed the cells at a 1:1 ratio, and injected them into recipient mice that had been immunized with OVA-loaded BMDCs 1 day before the experiment (Fig. 4D). The proportional contribution of each donor cell type to the total population of cells was determined at various time points by flow cytometric analysis (Fig. 4D). Both types of donor cells proliferated in the recipient mice, reaching their peak numbers on day 4, after which they declined (Fig. 4E). However, although both types of donor cells proliferated with similar kinetics, their respective proliferative capacities were different. The proportions of PKCη$^{+/+}$ and PKCη$^{-/-}$ T cells within the donor population started to diverge on day 1 (Fig. 4F). This difference in proportions increased over time, peaking at day 3, at which point the percentages of wild-type and PKCη$^{-/-}$ T cells were 69% versus 30%. This difference in cellular proportions was maintained until the end of the experiment. The differences in the proportion of PKCη$^{+/+}$ T cells to PKCη$^{-/-}$ T cells could have occurred because of differential cell death between the populations. To test this possibility, we incubated donor cells labeled with annexin V to detect cell surface phosphatidylserine (which is present on early apoptotic cells) and the DNA-intercalating dye 7-AAD (7-aminoactinomycin D) to distinguish viable from dying cells. Both PKCη$^{+/+}$ and PKCη$^{-/-}$ T cells had a small and roughly equal subset of dying cells (fig. S7), which suggested that differential cell death was unlikely to contribute to the difference in cellular proportions observed earlier (Fig. 4F). Collectively, these data indicate that the PKCη$^{-/-}$ CD8$^+$ T cells had a defect in the proliferative response to TCR stimulation, although the defect that was observed in assays in vitro was milder than that seen in PKCθ$^{-/-}$ T cells.

Ca^{2+} and NF-κB signaling in PKCη-deficient T cells are defective

The proliferative defect in PKCη$^{-/-}$ T cells could be a result of insufficient production of the cytokine IL-2, a prosurvival factor for T cells, deficient synthesis of the α chain of the IL-2 receptor (IL-2Rα, also known as CD25), or both, as occurs in PKCθ$^{-/-}$ T cells (*14*, *16*). In PKCη$^{-/-}$ CD8$^+$ cells, the increase in the cell surface abundance of CD25 was substantially reduced compared to that in wild-type CD8$^+$ cells, similar to the reduction observed in PKCθ$^{-/-}$ T cells (*16*) (Fig. 5A), as was the increase in abundance of the early activation marker CD69 (Fig. 5B). Because CD4$^+$ T cells are the main source of IL-2, we measured the amount of IL-2 secreted by PKCη$^{-/-}$ CD4$^+$ T cells and found that it was slightly (but significantly) reduced compared to that of wild-type CD4$^+$ T cells (fig. S8A).

NF-κB and Ca^{2+} signaling pathways are defective in PKCθ$^{-/-}$ mice, whereas TCR-proximal and mitogen-activated protein kinase (MAPK) signaling pathways are intact (*14*, *16*, *20*). We therefore investigated these pathways to try to determine the potential mechanisms responsible for the defects that we observed in PKCη$^{-/-}$ T cells. To measure changes in Ca^{2+} flux, we mixed wild-type (Thy1.1$^+$) and PKCη$^{-/-}$ (Thy1.2$^+$) T cells, loaded them with the Ca^{2+}-indicator dye Indo-1, and stimulated their TCRs by cross-linking prebound antibodies against CD3. In the PKCη-sufficient CD8$^+$ T cells, we observed a transient peak of increased Ca^{2+} followed by a sustained, gradually declining Ca^{2+} signal. In PKCη$^{-/-}$ CD8$^+$ T cells, the magnitude of the Ca^{2+} signal was reduced. This difference in Ca^{2+} signaling was not because of differential Indo-1 loading, because both cell types exhibited equivalent signals when stimulated with the Ca^{2+} ionophore ionomycin (Fig. 5C). Ca^{2+} signaling includes both the release of Ca^{2+} from endoplasmic reticulum (ER) stores and the subsequent induction of store-operated Ca^{2+} entry (SOCE) through channels in the plasma membrane (*27*). To identify at which stage Ca^{2+} signals were affected in PKCη$^{-/-}$ T cells, we measured Ca^{2+} flux in cells incubated with EGTA, which chelates extracellular Ca^{2+}, thus enabling us to measure only ER-dependent Ca^{2+} release, and in cells that were subsequently replenished with extracellular Ca^{2+}, thus enabling us to measure SOCE. These experiments showed no defect in ER-dependent Ca^{2+} release but did reveal a defect in SOCE in PKCη$^{-/-}$ T cells (Fig. 5D). We then directly compared Ca^{2+} signaling in PKCη$^{-/-}$ CD8$^+$ T cells and PKCθ$^{-/-}$ CD8$^+$ T cells and found a similar defect (fig. S8B).

The translocation of the NF-κB p65 subunit from the cytosol to the nucleus is a hallmark event in the NF-κB signaling cascade. We stimulated purified CD8$^+$ T cells with cross-linked antibodies against CD3 and CD8 and imaged the nuclear and cytoplasmic localization of p65. We observed translocation of p65 to the nucleus of 40% of wild-type cells, but only in 22% of PKCθ$^{-/-}$ T cells, whereas only 15% of PKCη$^{-/-}$ T cells showed nuclear translocation of p65 (Fig. 5, E and F). This result was further confirmed by Western blotting analysis of cytosolic and nuclear extracts. In wild-type CD8$^+$ T cells, nuclear p65 was increased in abundance for at least 60 min after stimulation, but in PKCη$^{-/-}$ T cells, the increase in the

Downloaded from stke.sciencemag.org on December 15, 2011

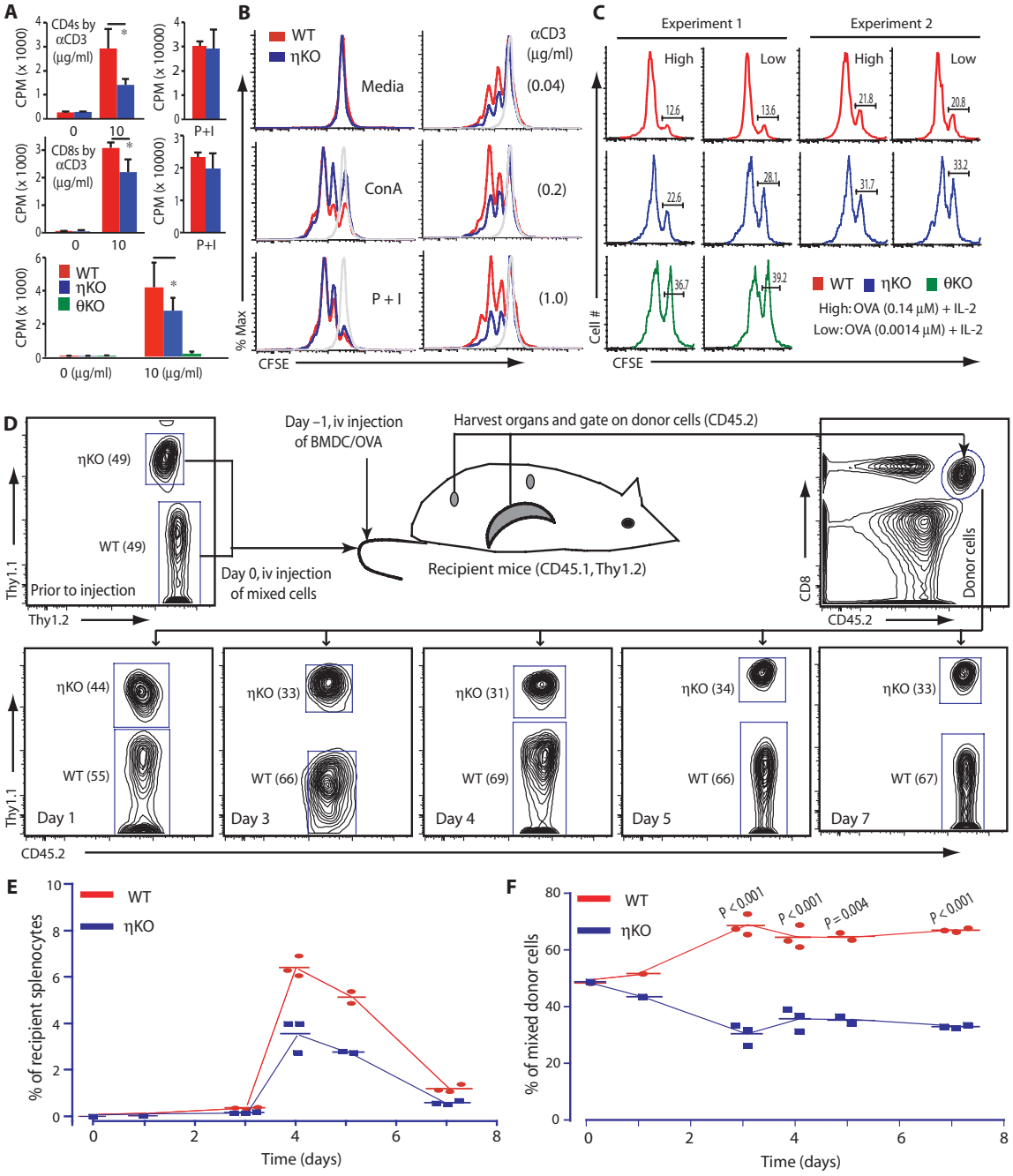

Fig. 4. Proliferation of PKCη$^{-/-}$ mature T cells is impaired. (**A**) Naïve T cells were stimulated with antibody against CD3 or with PMA and ionomycin (P + I) for 64 hours, and [^{3}H]thymidine was added to the culture medium for the last 16 hours. Graph shows proliferation as mean counts per minute (CPM) of ^{3}H incorporated into DNA ± SD of replicates ($n \geq 3$). (**B**) Lymph node cells from WT (CD45.1$^+$) and PKCη KO (CD45.2$^+$) mice were mixed, labeled with CFSE, and stimulated as indicated for 48 hours. Dilution of CFSE was analyzed by flow cytometry after gating for CD45 allotype and CD8. (**C**) OT-I TCR transgenic (Tg) WT (CD45.2$^+$Thy1.1$^+$) and PKCη$^{-/-}$ or PKCθ$^{-/-}$ (both CD45.2$^+$Thy1.2$^+$) naïve T cells were purified, mixed in a 1:1 ratio, labeled with CFSE, and stimulated with irradiated splenocytes (CD45.1$^+$) that were pulsed with OVA peptide. After 48 hours, CFSE dilution was analyzed by flow cytometry. The percentages of undivided cells are indicated for two independent experiments. (**D**) Antigen-specific proliferation of PKCη$^{-/-}$ T cells is impaired in vivo. Experiments were designed as depicted in the cartoon. Flow cytometry plots show the proportions of WT and KO donor cells that were present at the indicated times. iv, intravenous. (**E** and **F**) Proportions of WT and PKCη KO donor cells (E) per recipient mouse spleen and (F) within the donor cell population. Each dot in (E) and (F) represents an individual mouse. *$P \leq 0.05$. Data represent three (A) or four [(B) and (D to F)] independent experiments.

Downloaded from stke.sciencemag.org on December 15, 2011

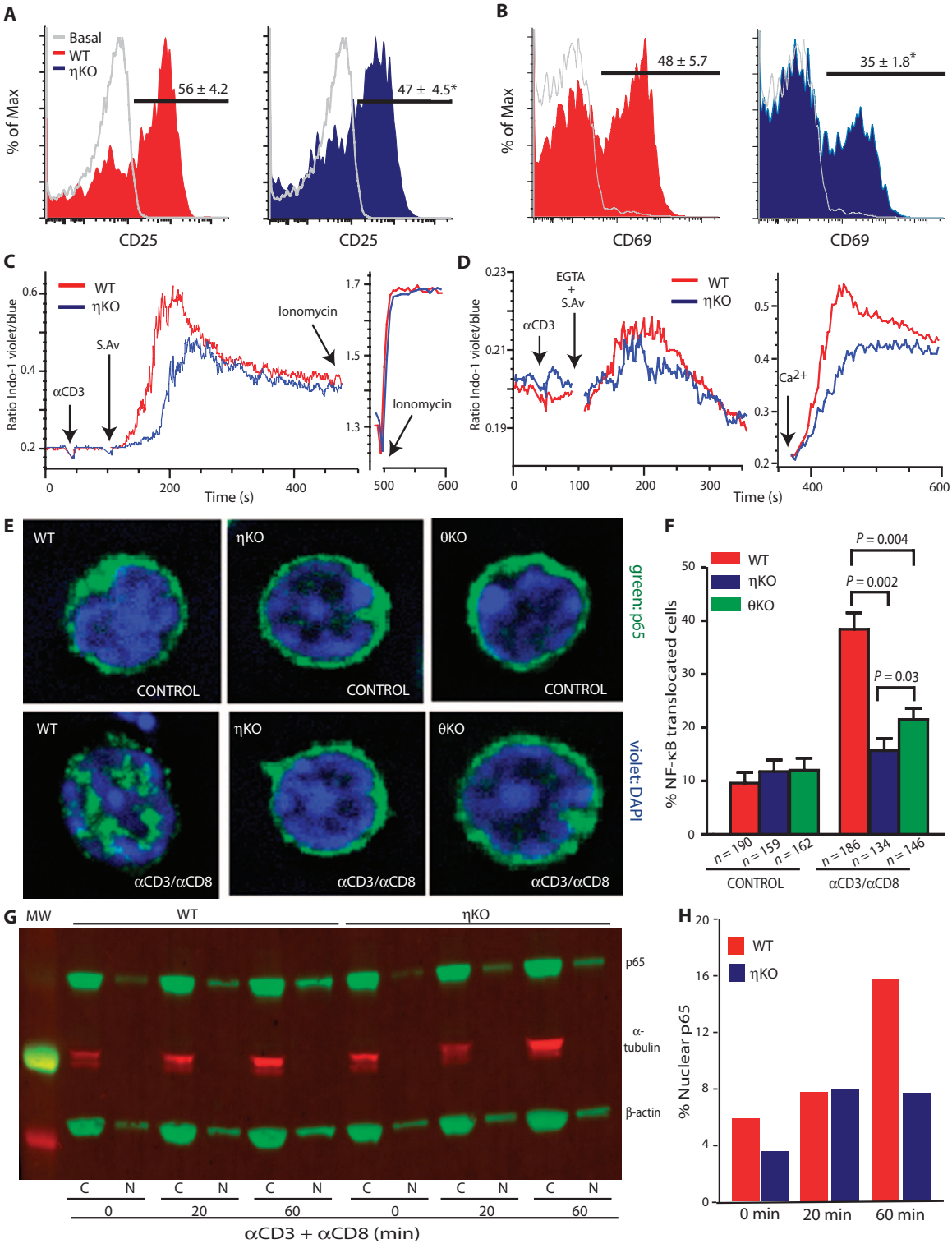

Fig. 5. Impaired signaling in mature PKCη$^{-/-}$ T cells. (A and B) Surface expression of activation markers. Lymph node cells were activated by stimulation with antibody against CD3 for 16 hours, and the surface abundance of (A) CD25 and (B) CD69 was analyzed on CD8^{+} cells by flow cytometry. The gray line indicates the basal abundance of these markers on nonstimulated cells, whereas the color-hatched region represents stimulated cells. CD25^{+} and CD69^{+} cell populations are marked and the mean percentages ± SD are shown. The asterisk indicates statistically significant difference (by *t* test) between KO and WT mice (n = 3 mice); P = 0.05 for CD25 and P < 0.05 for CD69. (C and D) Analysis of Ca^{2+} signaling. Cells from WT (Thy1.1^{+}) and PKCηKO (Thy1.2^{+}) mice were mixed, loaded with Indo-1, and stimulated by cross-linking biotinylated antibody against CD3 (αCD3) with streptavidin (S.Av). Ca^{2+} flux was recorded by flow cytometry. (E and F) Imaging of the nuclear translocation of NF-κB p65 protein. Purified CD8^{+} T cells were stimulated with antibodies against CD3 (αCD3) and CD8 (αCD8) for 60 min, and the nuclear translocation of p65 was determined by microscopy as shown in (E), and summarized in (F). (G and H) Examination of the nuclear translocation of p65 by Western blotting analysis. Cells were stimulated as shown in (E) and (F), after which cytosolic and nuclear extracts were prepared and subjected to Western blotting analysis (G). Normalized data are shown (H). Data represent two [(A), (B), (G), and (H)] or four [(C) to (F)] experiments.

Downloaded from stke.sciencemag.org on December 15, 2011

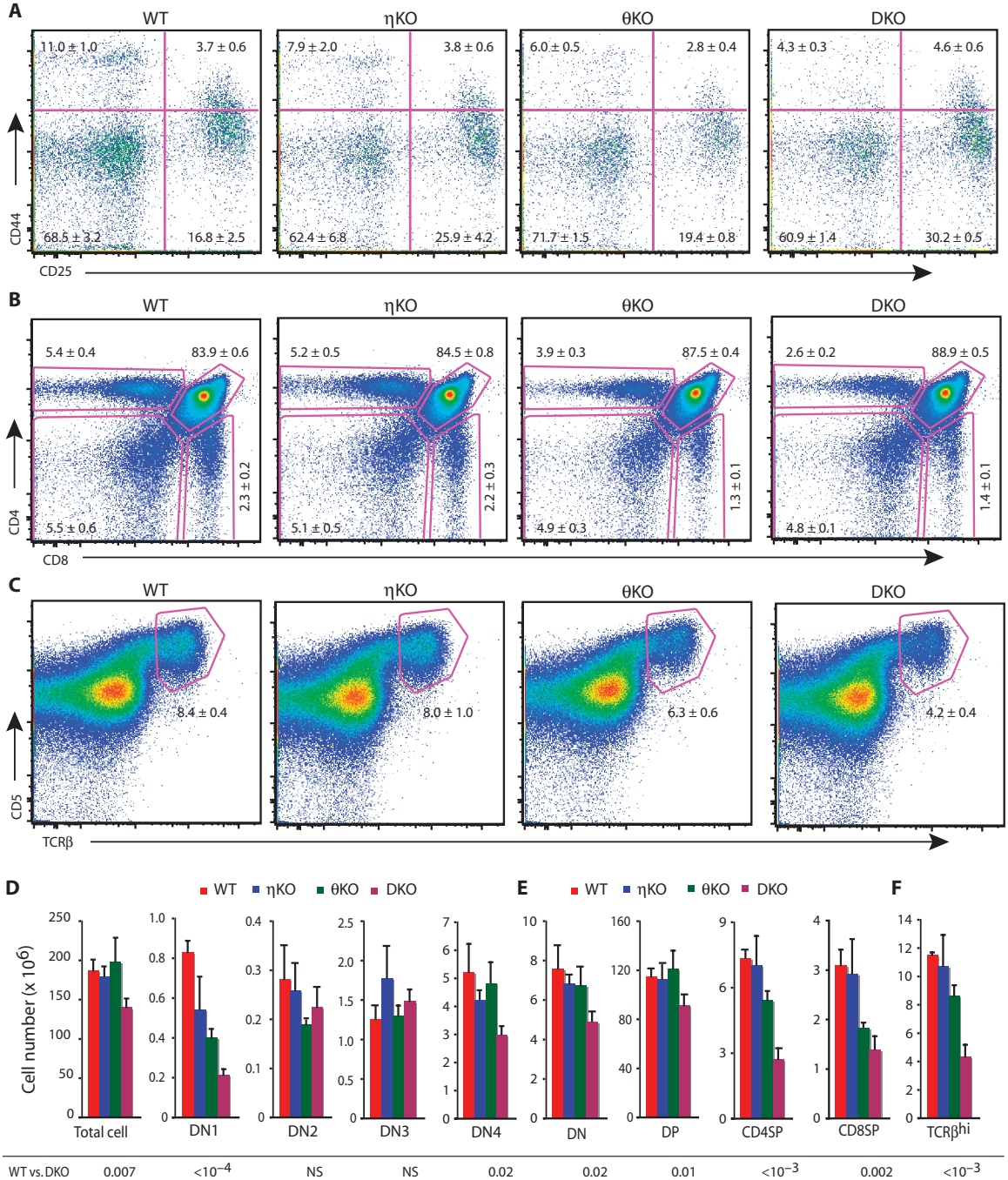

	Total cell	DN1	DN2	DN3	DN4	DN	DP	CD4SP	CD8SP	TCRβ^{hi}
WT vs. DKO	0.007	$<10^{-4}$	NS	NS	0.02	0.02	0.01	$<10^{-3}$	0.002	$<10^{-3}$
WT vs. ηKO	NS	0.04	NS	NS	NS	NS	NS	NS	NS	NS
WT vs. θKO	NS	$<10^{-3}$	NS	NS	NS	NS	NS	0.002	0.003	0.003
θKO vs. DKO	0.03	0.003	NS	NS	0.01	0.03	0.03	0.002	0.05	0.003

Fig. 6. Comparison of thymic phenotypes in three PKC-deficient mouse strains. Three age- and sex-matched mice from each genotype were used in this analysis. (**A** to **F**) Representative flow cytometry plots of (A) DN1 to DN4 stage thymocytes, (B) DN, DP, and SP stage thymocytes, and (C) the most mature CD5^{hi}TCR^{hi} thymocytes are shown with the proportions of each cell type listed as mean ± SD. Absolute cell numbers for each subset are listed in (D), (E), and (F), respectively. *P* values were calculated with the Student's *t* test and are listed underneath as indicated. Data represent three experiments.

Downloaded from stke.sciencemag.org on December 15, 2011

abundance of nuclear p65 ceased 20 min after stimulation (Fig. 5, G and H). The total amount of cellular p65 was not altered in PKCη$^{-/-}$ T cells (fig. S8C). Together, these results demonstrated that the NF-κB pathway was disrupted in the absence of PKCη at least as much as in the absence of PKCθ. TCR-proximal signaling and MAPK signaling pathways were normal in PKCη$^{-/-}$ T cells (fig. S8, D and E). Collectively, these results showed that PKCη$^{-/-}$ T cells were defective for Ca^{2+} and NF-κB signaling, which were also adversely affected in PKCθ$^{-/-}$ T cells.

DKO mice reveal isoform-specific and redundant roles for PKCη and PKCθ

The normal T cell development but the defective Ca^{2+} and NF-κB signaling pathways seen in PKCη$^{-/-}$ and PKCθ$^{-/-}$ mice prompted us to investigate a possible redundancy between PKCη and PKCθ in T cell development and function. To do this, we bred *Prkcq*$^{-/-}$, *Prkch*$^{-/-}$ DKO mice. In the thymus, DKO mice had a more substantial reduction in the numbers of DN1 and DN4 thymocytes than were observed in either of the single-knockout mice (Fig. 6, A and D). At the mature SP stage, although PKCθ$^{-/-}$ mice showed a mild defect in positive selection, the DKO mice had the most marked defect (Fig. 6, B and E). Thus, comparing the PKCθ$^{-/-}$ and DKO mice revealed a redundant role for PKCη in positive selection. This finding was confirmed when we analyzed the most mature population of cells in the thymus, the CD5^{hi}TCR^{hi} cells (Fig. 6C). No difference was noted between PKCη$^{-/-}$ and wild-type B6 mice, but the minor defect in thymocyte development in PKCθ$^{-/-}$ mice (*21*) was exacerbated by concomitant loss of PKCη (Fig. 6, C and F). Collectively, these findings demonstrated redundancy between PKCη and PKCθ; PKCη could substitute for PKCθ during positive selection, as was initially suggested by the increased abundance of PKCη and its recruitment to the immunological synapse in PKCθ$^{-/-}$ thymocytes (Fig. 1).

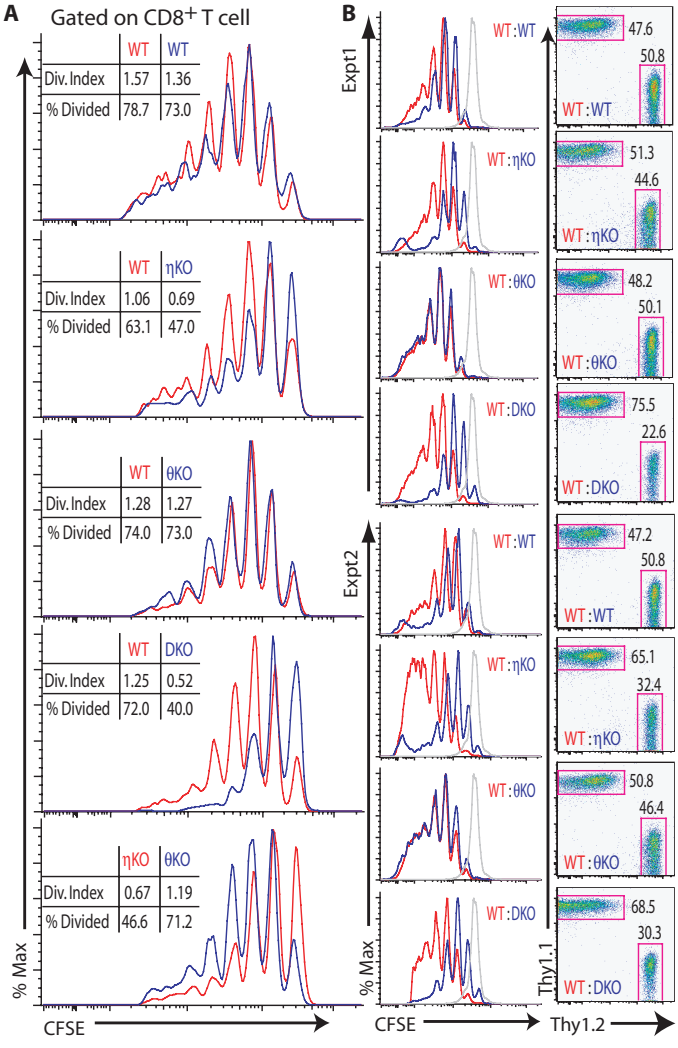

Fig. 7. Comparison of homeostatic proliferation in three PKC-deficient mouse strains. (A and B) Homeostatic proliferation assays were performed with (A) naïve polyclonal T cells or (B) naïve OT-I TCR Tg T cells as donor cells. Insets in each histogram in (A) show the parameters of division index and the percentages of divided cells as calculated with FlowJo software. The gray line in (B) shows undivided donor cells from nonirradiated mice. Results shown are one (A) or two (B) from four experiments.

We performed a comprehensive analysis of the lymph nodes and spleens of B6 mice and the various PKC knockout strains (fig. S9). Although redundancy between PKCη and PKCθ was apparent in thymocyte development, we observed an isoform-specific phenotype in mature T cells in the lymph nodes. For example, DKO mice and normal B6 mice had the same total number of T cells, as well as similar numbers of CD4^{+} and CD8^{+} T cell subsets. In contrast, PKCη$^{-/-}$ and PKCθ$^{-/-}$ mice had the highest and lowest number of these subsets, respectively (fig. S9B). More evidence supporting an isoform-specific role for PKCη in the biology of peripheral T cells came from analysis of the ratio of CD4^{+} to CD8^{+} cells in wild-type B6 mice and PKC-deficient strains of mice (fig. S9E). The CD4/CD8 T cell ratio was highest in PKCη$^{-/-}$ mice (lymph nodes: 1.69 ± 0.29; spleen: 2.39 ± 0.47) and lowest in PKCθ$^{-/-}$ mice (lymph nodes: 1.04 ± 0.12; spleen: 1.31 ± 0.21), with wild-type mice exhibiting intermediate ratios (lymph nodes: 1.44 ± 0.31; spleen: 1.87 ± 0.53). The biased CD4/CD8 ratios seen in single PKC knockout mice were "corrected" in DKO mice (lymph nodes: 1.53 ± 0.34; spleen: 1.88 ± 0.39). Together, these results strengthen the notion that PKCη and PKCθ have both redundant and isoform-specific roles in T cell development.

To determine whether the redundancy between PKCη and PKCθ was also manifested in T cell function, we measured the ability of T cells from the various PKC knockout mice to undergo homeostatic proliferation in vivo. T cell homeostatic proliferation occurs in response to a lymphopenic environment and is driven by TCR signaling (*26*). We sorted naïve T cells from wild-type (Thy1.1^{+}) and the different PKC knockout mice (all Thy1.2^{+}), mixed them at a 1:1 ratio, labeled them with CFSE, and injected them into sublethally irradiated recipient mice. One week later, we determined the CFSE staining of donor T cells by flow cytometry. We found that PKCη$^{-/-}$ CD8^{+} cells proliferated less well than did wild-type cells, with the most severe proliferation defect seen in DKO cells. PKCθ$^{-/-}$ cells showed no noticeable defect in proliferation compared to that of wild-type cells (Fig. 7A). That the homeostatic proliferation of DKO T cells was not completely abolished and that PKCη$^{-/-}$, but not PKCθ$^{-/-}$, CD8^{+} T cells had a noticeable proliferative defect was surprising. It was possible that the use of polyclonal donor T cells in these experiments obscured a defect in the PKC-deficient cells. Therefore, we repeated this experiment with MHC class I–restricted OT-I TCR transgenic T cells as the donor cells. The DKO cells proliferated poorly compared to the wild-type cells in recipient mice (Fig. 7B, left). We also observed a proliferative defect in the PKCη$^{-/-}$ cells, but not in the PKCθ$^{-/-}$ cells, consistent with the earlier experiments. We also analyzed the proportions of wild-type and PKC-deficient donor cells present in the recipient mice after 1 week. Although all of the cell combinations started at a 1:1 ratio, the proliferation of DKO cells was outpaced by that of wild-type T cells (Fig. 7B, right). PKCη$^{-/-}$ cells also represented a reduced

Downloaded from stke.sciencemag.org on December 15, 2011

Table 1. Comparison of PKCθ$^{-/-}$, PKCη$^{-/-}$, and DKO mice. ND, not determined; WT, wild type; Tg, transgenic; IS, immunological synapse.

	PKCθ KO	PKCη KO*	DKO*
Thymocytes			
Positive selection	Mildly impaired*	Normal	Strongly impaired
Negative selection	Normal	Normal	ND
Mature T cells			
CD4/CD8 T cell ratio	Lower than WT	Higher than WT	Equal to WT
Proliferation			
to αCD3 in vitro	Severely impaired	Mildly impaired	≈PKCθ KO
to PMA/ionomycin	Normal	Normal	ND
to antigen in vivo	Normal or impaired	Impaired	ND
to antigen in vitro	Impaired	Impaired	ND
Homeostatic proliferation			
Non-Tg	CD8 normal	CD8 impaired	Strongly impaired
OT-I Tg	Normal*	Impaired	Strongly impaired
Signaling events			
Ca^{2+} flux	Impaired	Impaired	ND
NF-κB translocation	Impaired	Impaired	ND
Recruitment to IS†	Recruited, central region	Recruited, diffuse pattern	

*Based on data obtained from this study. †Not based on knockout mice.

proportion of the cell population after a week, but the proportion of PKCθ$^{-/-}$ cells was similar to that of the wild-type cells. These changes matched the data from the CFSE-labeling experiments, demonstrating that PKCη, not PKCθ, played a major role in the homeostatic proliferation of CD8$^+$ T cells. In addition to TCR signaling, cytokines such as IL-7 and IL-15 can also promote homeostatic proliferation; however, altered responsiveness to these cytokines during homeostatic proliferation seems unlikely in the case of PKCη$^{-/-}$ and DKO T cells, because the amounts of IL-7Rα (CD127) and IL-15R (CD122) on the surface of these cells was comparable to those of wild-type T cells (fig. S10).

DISCUSSION

The finding that the abundance of PKCη mRNA was increased during the positive selection of thymocytes (*6*, *7*) was surprising, given the widely accepted importance of PKCθ in T cell biology, in particular that PKCθ is recruited to the central region of the immunological synapse (*9*, *10*). PKCη was also recruited to the immunological synapse during thymocyte development and in mature T cells. PKCη formed a diffuse pattern at the immunological synapse, such that although PKCη and PKCθ were co-recruited to the immunological synapse, PKCθ is concentrated at the central synapse, but PKCη was not. Such different localization patterns might lead to different functions. This suggestion is consistent with our data showing that T cell activation involving immunological synapse formation (antigen-specific proliferation in response to APCs) was more severely affected in cells lacking PKCη than were responses that did not involve an immunological synapse, such as stimulation with antibody against CD3 or with a combination of phorbol 12-myristate 13-acetate (PMA) and ionomycin.

Knockout mice have been powerful tools in immunological studies, as evidenced by the studies of PKCθ in T cell biology (*14*, *16*). In contrast, studies on PKCη have lagged behind. The first study of a PKCη knockout mouse was published several years ago but lacked any immunological analysis (*8*). Until now, there has been no follow-up study of this or any other PKCη knockout mouse. We have summarized the similarities and differences between PKCη$^{-/-}$, PKCθ$^{-/-}$, and the DKO mice on the basis of this study and work from others (Table 1) (*14*, *16*, *20*, *21*).

That thymocyte development was normal in PKCη$^{-/-}$ mice was not unexpected. Initial reports on PKCθ$^{-/-}$ mice did not identify any defects in thymocyte development despite showing severely impaired mature T cell function (*14*, *16*); however, a study reexamining thymocyte development in PKCθ$^{-/-}$ mice showed a mild deficiency (*21*), which is also in agreement with our observations here. Therefore, it is possible that the lack of obvious developmental or functional defects in any single PKC knockout mouse strain results from a redundancy between PKC isoforms, especially those members within the same subfamily. This is evidenced in our PKCη$^{-/-}$PKCθ$^{-/-}$ DKO mice, in which positive selection was more severely impaired than in either single-knockout mouse.

Although redundancy between different PKC isoforms obscures some roles of individual PKC isoforms, we did find clear individual roles for PKCη in this study. For example, a reduced homeostatic proliferation of CD8$^+$ T cells (either polyclonal or OT-I TCR transgenic T cells) was seen only in PKCη$^{-/-}$ cells, but not in PKCθ$^{-/-}$ cells. Also, PKCη$^{-/-}$ mice had a higher ratio of CD4$^+$ T cells to CD8$^+$ T cells than did wild-type mice, whereas PKCθ$^{-/-}$ mice had a lower ratio. Knockout of both PKC isoforms resulted in a CD4/CD8 T cell ratio that was similar to that of wild-type mice. Previous work has shown that the ratio of CD4$^+$ to CD8$^+$ T cells is influenced by a number of factors during development (*28*–*30*); however, the effect of PKC knockout that we observed appeared to occur post-thymically, because SP thymocytes from the knockout mice did not show altered ratios of CD4$^+$ to CD8$^+$ T cells. Together, these results demonstrate PKCη-specific roles in T cells.

The enlarged lymph nodes seen in PKCη$^{-/-}$ mice relative to those of wild-type mice were also noted in PKCδ$^{-/-}$ animals (*31*) but were not observed in PKCθ$^{-/-}$ mice (*14*, *16*). In PKCδ$^{-/-}$ mice, lymphadenopathy was associated with increased numbers of B cells as well as a marked increase in the ratio of B cells to T cells (*31*). However, the situation in PKCη$^{-/-}$ mice was more complicated. In the lymph nodes, the relative proportions of B cells and T cells were barely different (~4% difference) and thus were unlikely to account for the substantially increased cell numbers (40 to 50%) in the lymph nodes of the PKCη$^{-/-}$ mice compared to those of normal mice. In contrast, in the spleens of PKCη$^{-/-}$ mice, the numbers of B cells and T cells were reduced compared to those in spleens from wild-type mice. We speculate that the differences in lymphocyte numbers between the lymph nodes and the spleens of the PKCη$^{-/-}$ mice may reflect altered lymphocyte homing, homeostasis, or both and are worth further investigation. We found that Ca^{2+} flux and NF-κB translocation were impaired in PKCη$^{-/-}$ T cells, but that TCR-proximal tyrosine phosphorylation events and MAPK signaling pathways were intact. These signaling

Downloaded from stke.sciencemag.org on December 15, 2011

defects are similar to those of PKCθ$^{-/-}$ T cells. Unlike PKCθ, about which there are many in-depth studies on the molecular signaling machinery (*15*, *18–20*), the investigation of PKCη is still at an early stage.

One puzzle raised in this and other studies is that there is an apparent discrepancy between the severe defect seen in PKCθ$^{-/-}$ T cells in studies in vitro and the mostly mild (if any) defect observed in studies in vivo. For example, the absence of PKCθ impairs the differentiation of T helper type 2 (T_H2) cells but not that of T_H1 cells, which results in reduced immune responses against *Leishmania major* (*32*). Similarly, PKCθ deficiency results in impaired responses to *Listeria monocytogenes* infection (*33*), but not to impaired antiviral immune responses (*34*, *35*). As we showed here, PKCθ$^{-/-}$ CD8$^+$ T cells showed normal homeostatic proliferation, whereas this was impaired in PKCη$^{-/-}$ CD8$^+$ T cells. Thus, the deficiencies seen in PKCη$^{-/-}$ T cells in vivo were more marked than those of PKCθ$^{-/-}$ T cells. It will be interesting to determine how PKCη$^{-/-}$ and DKO T cells behave in vivo in response to viral and bacterial infections.

We have demonstrated that PKCη has specific as well as redundant (with PKCθ) functions in T cell biology, which are separated by developmental stage. Although redundant during T cell development, specific roles for PKCη in the responsiveness of CD8$^+$ T cells were apparent in the periphery. Deficiencies in CD8$^+$ T cell responses to peptide-MHC complex may cause the increased CD4/CD8 T cell ratio in peripheral T cells that we observed in the PKCη$^{-/-}$ mice. In addition, PKCη was required to balance the distribution of lymphocytes between different lymphoid organs. Together, these factors point to the importance of PKCη in T cell biology.

MATERIALS AND METHODS

Mice

B6.PL-*Thy1a*/CyJ (Thy1.1$^+$CD45.2$^+$) and B6.SJL-*Ptprca Pepcb*/BoyJ (Thy1.2$^+$CD45.1$^+$) mice were purchased from Jackson Laboratories. C57BL/6 (Thy1.2$^+$CD45.2$^+$) mice were bred at The Scripps Research Institute (TSRI). OT-I and OT-I *Tap*$^{-/-}$ animals were obtained from S. Jameson and K. Hogquist (University of Minnesota, Minneapolis, MN), and *Prkcq*$^{-/-}$ mice (*14*) and OT-I *Prkcq*$^{-/-}$ were provided by A. Altman (La Jolla Institute for Allergy and Immunology). *Prkch*$^{-/-}$ mice were generated in this study. All experiments were performed in accordance with the guidelines of the Animal Care and Use Committee of TSRI.

Antibodies, cytokines, and reagents

Antibodies against CD3 (145-2C11), CD4 (RM4.4, RM4.5, GK1.5), CD8α (53-6.7), CD25 (PC61.5), CD62L (MEL14), CD44 (IM7), Vβ5 (MR9-6), Vβ6 (RR4-7), Vβ11 (CTVB11), and Vβ12 (CTVB12b) were obtained from eBioscience, BioLegend, or BD Biosciences. Antibodies against phosphorylated extracellular signal–regulated kinase 1 and 2 (ERK1/2) (T^{202}/Y^{204}, clone 197G2), phosphorylated p38 MAPK (Thr^{180}/Tyr^{182}, clone 3DT), α-tubulin, and β-actin were from Cell Signaling Technology. Antibodies against p65, PKCη, and PKCθ were obtained from Santa Cruz Biotechnology. Recombinant IL-3, IL-6, and stem cell factor were obtained from PeproTech. Granulocyte macrophage colony-stimulating factor was generated as described previously (*36*). Streptavidin was obtained from Jackson ImmunoResearch Laboratories. The GeneJammer transfection reagent was from Stratagene. The AmiconUltra centrifugal filter device (UFC810024) was obtained from Millipore. EasySep Mouse total T cell, CD4$^+$, and CD8$^+$ T Cell Negative Enrichment Kits were from STEMCELL Technologies. Indo-1 AM and CFDA-SE (CFSE) were from Molecular Probes (Invitrogen).

Real-time RT-PCR

Total RNA from the thymi of 4- to 8-week-old OT-I mice or from sorted subpopulations was isolated with the RNeasy Mini Kit (Qiagen). The RNA was treated with deoxyribonuclease I (DNase I; Invitrogen) for 15 min at room temperature. The reaction was stopped by the addition of 25 mM EDTA, and the DNase was inactivated by incubating the samples at 65°C for 10 min. RNA samples were used as templates to synthesize complementary DNA (cDNA) with the SuperScript First-Strand Synthesis System for RT-PCR (Invitrogen) according to the manufacturer's recommendations. Oligonucleotide primers were designed with Primer Express 1.5 software (PE Applied Biosystems). The primer sequences are as follows: PKCη 5′ primer: 5′-CTCCAGACCGTCTGTTCTTTGTC-3′; 3′ primer: 5′-ATCTCCGCGGCGTAGAAA-3′; GenBank accession number D90242; ribosomal protein 5′ primer: 5′-AGATGCAGCAGATCCGCAT-3′; 3′ primer: 5′-GGATGGCCTTGCGCA-3′; GenBank accession number BC011106. Real-time PCR reactions were performed on the ABI Prism 7700 Sequence Detection System with SYBR Green PCR Master Mix (PE Applied Biosystems). The PCR mix was optimized for SYBR Green reactions and contained SYBR Green 1 dye, AmpliTaqGold DNA polymerase, and deoxynucleotide triphosphates (dNTPs) with deoxyuridine triphosphate (dUTP). Each reaction was performed in a final volume of 25 μl and contained the SYBR Green PCR Master Mix, cDNA, and 150 nM of each primer. Two independent experiments were performed, and all reactions were performed in duplicate. A standard curve with a twofold serial dilution of the standard cDNA was generated for the target gene as well as for the housekeeping gene ribosomal protein. cDNAs (20 ng per reaction) from the different cell populations were used as templates for real-time PCR. Standard curves were used to determine the relative concentrations of amplified transcripts. The amounts of PKCη mRNA were first normalized to those of the ribosomal protein mRNA. The normalized sample values were finally divided by the normalized amounts of PKCη mRNA in samples from OT-I TCR^{lo} DP cells to obtain the fold change in mRNA abundance between the different populations of DP thymocytes.

Generation of PKCη$^{-/-}$ mice

The strategy for generating PKCη knockout mice was as described previously (fig. S5) (*37*) except that all cloning materials, embryonic stem cell line (Bruce4), and founder mice used for breeding were on a B6 background. PKCθ knockout mice were described previously (*14*) and were maintained in TSRI animal facility by further breeding onto the B6 background. DKO mice were generated by breeding PKCη$^{-/-}$ and PKCθ$^{-/-}$ mice together.

T cell activation and proliferation assays

Purified naïve CD8$^+$ T cells from mice were used in experiments as indicated in the text. Purification was performed with biotinylated antibodies in conjunction with magnetic beads conjugated with antibodies against biotin (BD Biosciences), or cells were sorted with a flow cytometer. Cells were stimulated with plate-bound or soluble antibody against CD3 as indicated in the figures, and cells were incubated with antibodies against CD69, CD25, CD4, and CD8 for flow cytometric analysis. Thymidine incorporation assays were performed as described (*14*). For proliferation assays involving CFSE dilution, lymphocytes were incubated with CFSE (0.2 μM) at 37°C for 10 min, which was stopped by the addition of 10 volumes of cRPMI [RPMI medium supplemented with 10% fetal calf serum (FCS), penicillin (100 U/ml), streptomycin (10 μg/ml), glutamine (292 μg/ml), 50 μM 2-mercaptoethanol, and 25 mM Hepes (pH 7.2 to 7.5)]. After washing, cells were cultured with or without antibody against CD3 in cRPMI for 48 hours or in the presence of irradiated B6.SJL-*Ptprca Pepcb*/BoyJ (CD45.1) splenocytes that had been pulsed with the indicated concentration

Downloaded from stke.sciencemag.org on December 15, 2011

of OVA peptide. T cell proliferation was determined by measuring the dilution of CFSE in cells by flow cytometry. For measurement of IL-2 production, $CD4^+$ T cells were purified from lymph nodes with the EasySep Mouse $CD4^+$ T Cell Enrichment Kit (STEMCELL), and 2×10^5 cells were seeded per well in a BioCoat T-Cell Activation Plate, which was precoated with antibody against CD3 (BD Biosciences). To stimulate cells, we added soluble antibody against CD28 to the cell culture medium to a final concentration of 1 μg/ml and incubated the cells at 37°C in 5% CO_2 for 48 hours. Culture supernatants were removed, and the concentration of IL-2 produced by the cells was measured with the mouse IL-2 enzyme-linked immunosorbent assay (ELISA) Ready Set Go kit (eBioscience) according to the manufacturer's instructions.

Ca^{2+} signaling

Ca^{2+} flux was performed as described previously (*37*, *38*). Briefly, lymphocytes were isolated from wild-type mice ($Thy1.1^+$ or $Thy1.2^+$) and $PKC\eta^{-/-}$ mice ($Thy1.2^+$). Cells from different genotypes were mixed at a 1:1 ratio. Cells were suspended at 2×10^6 to 5×10^6/ml in cRPMI and were incubated with 2 μM Indo-1 AM for 30 min at 37°C in 5% CO_2. Cells were washed twice with cRPMI and resuspended in 0.5 ml of cRPMI or cHBSS [Hanks' balanced salt solution (HBSS) supplemented with 1% FCS, 1 mM EGTA, 1 mM $MgCl_2$, and 10 mM Hepes (pH 7.2 to 7.5)]. Cells were prewarmed to 37°C before analysis and were kept at 37°C during event collection on a Becton-Dickinson LSR-II flow cytometer. To stimulate cells, we added reagents during the analysis as indicated in the figures. Maximal Ca^{2+} flux was obtained by addition of ionomycin (500 ng/ml; Calbiochem). The mean fluorescence ratio was calculated with FlowJo software (TreeStar).

Western blotting analysis

$CD8^+$ T cells were stimulated with cross-linking antibodies against CD3 and CD8 for the times indicated in the figures. Cell lysates were prepared, resolved by SDS–polyacrylamide gel electrophoresis (SDS-PAGE), and analyzed by Western blotting with the indicated antibodies, as described previously (*37*). To measure the nuclear translocation of NF-κB p65, we stimulated cells as described earlier, chilled the cells on ice, and fractionated them with the NE-PER kit (Pierce). Western blotting analysis of samples was performed with the Li-Cor Odyssey infrared imaging system. Normalization and calculation of fraction purity and the ratios of nuclear to cytosolic p65 abundance were performed according to Li-Cor protocols with p65, total protein, actin, and tubulin signals.

In vivo proliferation assays

Proliferation of OT-I TCR transgenic cells in response to stimulation with OVA peptide in vivo was measured as described previously (*39*). Briefly, OT-I TCR $CD8^+$ T cells were purified with a $CD8^+$ T cell Negative Enrichment Kit (STEMCELL). Wild-type ($Thy1.2^+CD45.2^+$) and $PKC\eta^{-/-}$ ($Thy1.1^+/Thy1.2^+CD45.2^+$) cells were mixed at a 1:1 ratio and transferred into recipient B6.SJL mice ($Thy1.2^+CD45.1^+$). The recipient mice were intravenously injected with BMDCs that had been pulsed with $OVA_{257–264}$ peptide 1 day before transfer of the T cells. At various time points, cells from the lymph nodes and spleens of recipient mice were collected, and the proportions and absolute cell numbers of donor cells were determined by flow cytometry. BMDCs were cultured and induced to maturation as described previously (*36*, *39*, *40*). Briefly, on day 7 of BMDC culture, lipopolysaccharide (100 ng/ml) was added overnight to induce maturation. BMDC maturity and phenotype were confirmed by flow cytometric analysis of the surface expression of CD11c, CD86, CD80, and MHC-II. The resultant cell population contained >90% $CD11c^+$ $MHC\text{-}II^{hi}$ BMDCs.

Homeostatic proliferation assays

Naïve T cells ($CD62L^+CD44^-$) were sorted from mice (all of which were $CD45.2^+$, but were either $Thy1.1^+$ or $Thy1.2^+$). $Thy1.1^+$ or $Thy1.2^+$ sorted cells were mixed in a 1:1 ratio, labeled with CFSE, and injected intravenously into recipient B6.SJL mice ($Thy1.2^+CD45.1^+$), which were sublethally irradiated (5.5 Gy) with a Gammacell 40 (MDS Nordion) before cell transfer. One week later, cells from the lymph nodes and spleens of recipient mice were collected and analyzed by flow cytometry.

Microscopy

To visualize the recruitment of PKC to the immunological synapse in live cells, we transfected T cell hybridomas with plasmid encoding fusion proteins of PKC isoforms and fluorescent proteins as indicated in the text. The form of RFP used was tdimer2(12) (*41*). APCs were loaded with peptides or superantigens as indicated in the figures. T cell hybridomas and APCs were mixed together for various time points and were fixed before imaging. For time-lapse imaging of T cell–APC conjugates (fig. S4), T cell hybridomas and APCs were sequentially loaded into an FCS2 flow chamber (Bioptechs) that was heated to 37°C. To visualize the recruitment of PKC to the immunological synapse in live primary T cells, we incubated 1×10^7 thymocytes with 2×10^7 EL4 cells that were pulsed with OVA peptide (10 mM) or with 2×10^7 LK35 B cell (class II^+) tumor cells presenting the superantigens SEA (50 ng/ml) and SEB (10 μg/ml; Toxin Technology) in 96-well, round-bottomed plates for 30 or 60 min at 37°C. Thymocytes were then fixed with 4% paraformaldehyde (PFA) for 12 min at room temperature. To detect cell surface markers, we incubated thymocytes with biotinylated antibodies against CD4, CD8, or LFA-1 (BD Biosciences) and then incubated them with Alexa Fluor 488–conjugated streptavidin (Molecular Probes). For intracellular staining, cells were permeabilized with 0.2% saponin for 15 min at room temperature. Cells were then incubated with rabbit antibodies against the appropriate PKC isoform, after which they were incubated with Alexa Fluor 568– or Alexa Fluor 680–conjugated antibodies against rabbit antibodies (Molecular Probes). To visualize the nuclear translocation of NF-κB in primary T cells, we purified 2×10^6 $CD8^+$ T cells from lymph nodes by magnetic negative selection and plated the cells on Lab-Tek II chambered cover glass coated with poly-L-lysine (Sigma). The cells were then stimulated with cross-linking antibodies against CD3 and CD8 for the times indicated in the figures. T cells were then fixed with 4% PFA for 12 min at room temperature. Cells were permeabilized with 0.3% Triton X-100 for 3 min at room temperature. Cells were then incubated with rabbit antibody against p65 (1 μg/ml), after which they were incubated with Alexa Fluor 488–conjugated secondary antibody against rabbit antibody (Molecular Probes). Nuclei were counterstained with the DNA binding dye 4′,6-diamidino-2-phenylindole (DAPI, Invitrogen). All images were captured with a Zeiss Axiovert 200 M inverted microscope. SlideBook software (Intelligent Imaging Innovations) was used for the capture as well as for deconvolution and image analysis, and ImageJ was used for image presentation.

Statistical analysis

Statistical differences were calculated with the mean difference hypothesis of Student's two-tailed *t* test, assuming different variances and a confidence level of 95%. Calculations were performed with Microsoft Excel.

SUPPLEMENTARY MATERIALS

www.sciencesignaling.org/cgi/content/full/4/202/ra84/DC1

Fig. S1. Recruitment of PKCη to the immunological synapse in the presence of PKCθ.

Fig. S2. Recruitment of PKCη to the immunological synapse in preselection thymocytes in the absence of PKCθ.

Fig. S3. Antigen-specific recruitment of PKCη to the immunological synapse.

Fig. S4. Time course of the recruitment of PKCη and PKCθ to the immunological synapse.

Downloaded from stke.sciencemag.org on December 15, 2011

Fig. S5. Generation of PKCη$^{-/-}$ mice.
Fig. S6. Analysis of CD4$^+$ T cell subsets.
Fig. S7. Cell death status of wild-type and PKCη KO cells responding to antigen in vivo.
Fig. S8. TCR signaling cascade in mature T cells from PKCη$^{-/-}$ mice.
Fig. S9. Comparison of peripheral T cell phenotypes in three PKC-deficient mouse strains.
Fig. S10. IL-7Rα (CD127) and IL-15R (CD122) abundances on PKC-deficient cells are normal.
References

REFERENCES AND NOTES

1. E. C. Dempsey, A. C. Newton, D. Mochly-Rosen, A. P. Fields, M. E. Reyland, P. A. Insel, R. O. Messing, Protein kinase C isozymes and the regulation of diverse cell responses. *Am. J. Physiol. Lung Cell. Mol. Physiol.* **279**, L429–L438 (2000).
2. N. Isakov, A. Altman, Protein kinase Cθ in T cell activation. *Annu. Rev. Immunol.* **20**, 761–794 (2002).
3. G. Baier, The PKC gene module: Molecular biosystematics to resolve its T cell functions. *Immunol. Rev.* **192**, 64–79 (2003).
4. K. Hayashi, A. Altman, Protein kinase C θ (PKCθ): A key player in T cell life and death. *Pharmacol. Res.* **55**, 537–544 (2007).
5. S. Manicassamy, S. Gupta, Z. Sun, Selective function of PKC-θ in T cells. *Cell. Mol. Immunol.* **3**, 263–270 (2006).
6. V. E. Mick, T. K. Starr, T. M. McCaughtry, L. K. McNeil, K. A. Hogquist, The regulated expression of a diverse set of genes during thymocyte positive selection in vivo. *J. Immunol.* **173**, 5434–5444 (2004).
7. N. Niederberger, L. K. Buehler, J. Ampudia, N. R. J. Gascoigne, Thymocyte stimulation by anti-TCR-β, but not by anti-TCR-α, leads to induction of developmental transcription program. *J. Leukoc. Biol.* **77**, 830–841 (2005).
8. K. Chida, T. Hara, T. Hirai, C. Konishi, K. Nakamura, K. Nakao, A. Aiba, M. Katsuki, T. Kuroki, Disruption of protein kinase Cη results in impairment of wound healing and enhancement of tumor formation in mouse skin carcinogenesis. *Cancer Res.* **63**, 2404–2408 (2003).
9. C. R. F. Monks, H. Kupfer, I. Tamir, A. Barlow, A. Kupfer, Selective modulation of protein kinase C-θ during T-cell activation. *Nature* **385**, 83–86 (1997).
10. C. R. F. Monks, B. A. Freiberg, H. Kupfer, N. Sciaky, A. Kupfer, Three-dimensional segregation of supramolecular activation clusters in T cells. *Nature* **395**, 82–86 (1998).
11. A. Grakoui, S. K. Bromley, C. Sumen, M. M. Davis, A. S. Shaw, P. M. Allen, M. L. Dustin, The immunological synapse: A molecular machine controlling T cell activation. *Science* **285**, 221–227 (1999).
12. T. Yokosuka, W. Kobayashi, K. Sakata-Sogawa, M. Takamatsu, A. Hashimoto-Tane, M. L. Dustin, M. Tokunaga, T. Saito, Spatiotemporal regulation of T cell costimulation by TCR-CD28 microclusters and protein kinase C θ translocation. *Immunity* **29**, 589–601 (2008).
13. K. L. Singleton, K. T. Roybal, Y. Sun, G. Fu, N. R. J. Gascoigne, N. S. van Oers, C. Wulfing, Spatiotemporal patterning during T cell activation is highly diverse. *Sci. Signal.* **2**, ra15 (2009).
14. Z. Sun, C. W. Arendt, W. Ellmeier, E. M. Schaeffer, M. J. Sunshine, L. Gandhi, J. Annes, D. Petrzilka, A. Kupfer, P. L. Schwartzberg, D. R. Littman, PKC-θ is required for TCR-induced NF-κB activation in mature but not immature T lymphocytes. *Nature* **404**, 402–407 (2000).
15. T. Egawa, B. Albrecht, B. Favier, M. J. Sunshine, K. Mirchandani, W. O'Brien, M. Thome, D. R. Littman, Requirement for CARMA1 in antigen receptor-induced NF-κB activation and lymphocyte proliferation. *Curr. Biol.* **13**, 1252–1258 (2003).
16. C. Pfeifhofer, K. Kofler, T. Gruber, N. G. Tabrizi, C. Lutz, K. Maly, M. Leitges, G. Baier, Protein kinase Cθ affects Ca^{2+} mobilization and NFAT cell activation in primary mouse T cells. *J. Exp. Med.* **197**, 1525–1535 (2003).
17. H. Hara, C. Bakal, T. Wada, D. Bouchard, R. Rottapel, T. Saito, J. M. Penninger, The molecular adapter Carma1 controls entry of IκB kinase into the central immune synapse. *J. Exp. Med.* **200**, 1167–1177 (2004).
18. D. Wang, R. Matsumoto, Y. You, T. Che, X. Y. Lin, S. L. Gaffen, X. Lin, CD3/CD28 costimulation-induced NF-κB activation is mediated by recruitment of protein kinase C-θ, Bcl10, and IκB kinase β to the immunological synapse through CARMA1. *Mol. Cell. Biol.* **24**, 164–171 (2004).
19. J. P. Roose, M. Mollenauer, V. A. Gupta, J. Stone, A. Weiss, A diacylglycerol-protein kinase C-RasGRP1 pathway directs Ras activation upon antigen receptor stimulation of T cells. *Mol. Cell. Biol.* **25**, 4426–4441 (2005).
20. S. Manicassamy, M. Sadim, R. D. Ye, Z. Sun, Differential roles of PKC-θ in the regulation of intracellular calcium concentration in primary T cells. *J. Mol. Biol.* **355**, 347–359 (2006).
21. S. C. Morley, K. S. Weber, H. Kao, P. M. Allen, Protein kinase C-θ is required for efficient positive selection. *J. Immunol.* **181**, 4696–4708 (2008).
22. M. J. Irwin, N. R. J. Gascoigne, Interplay between superantigens and the immune system. *J. Leukoc. Biol.* **54**, 495–503 (1993).
23. P. P. Yachi, J. Ampudia, N. R. J. Gascoigne, T. Zal, Nonstimulatory peptides contribute to antigen-induced CD8-T cell receptor interaction at the immunological synapse. *Nat. Immunol.* **6**, 785–792 (2005).
24. T. K. Starr, S. C. Jameson, K. A. Hogquist, Positive and negative selection of T cells. *Annu. Rev. Immunol.* **21**, 139–176 (2003).
25. M. T. Scherer, L. Ignatowicz, G. M. Winslow, J. W. Kappler, P. Marrack, Superantigens: Bacterial and viral proteins that manipulate the immune system. *Annu. Rev. Cell Biol.* **9**, 101–128 (1993).
26. J. Sprent, C. D. Surh, Normal T cell homeostasis: The conversion of naive cells into memory-phenotype cells. *Nat. Immunol.* **12**, 478–484 (2011).
27. K. Q. Liu, S. C. Bunnell, C. B. Gurniak, L. J. Berg, T cell receptor–initiated calcium release is uncoupled from capacitative calcium entry in Itk-deficient T cells. *J. Exp. Med.* **187**, 1721–1727 (1998).
28. H. Suzuki, J. A. Punt, L. G. Granger, A. Singer, Asymmetric signaling requirements for thymocyte commitment to the CD4$^+$ versus CD8$^+$ T cell lineages: A new perspective on thymic commitment and selection. *Immunity* **2**, 413–425 (1995).
29. P. Corbella, D. Moskophidis, E. Spanopoulou, C. Mamalaki, M. Tolaini, A. Itano, D. Lans, D. Baltimore, E. Robey, D. Kioussis, Functional commitment to helper T cell lineage precedes positive selection and is independent of T cell receptor MHC specificity. *Immunity* **1**, 269–276 (1994).
30. B.-C. Sim, N. Aftahi, C. Reilly, B. Bogen, R. H. Schwartz, N. R. J. Gascoigne, D. Lo, Thymic skewing of the CD4/CD8 ratio maps with the T-cell receptor α-chain locus. *Curr. Biol.* **8**, 701–704 (1998).
31. I. Mecklenbräuker, K. Saijo, N. Y. Zheng, M. Leitges, A. Tarakhovsky, Protein kinase Cδ controls self-antigen-induced B-cell tolerance. *Nature* **416**, 860–865 (2002).
32. B. J. Marsland, T. J. Soos, G. Spath, D. R. Littman, M. Kopf, Protein kinase Cθ is critical for the development of in vivo T helper (Th)2 cell but not Th1 cell responses. *J. Exp. Med.* **200**, 181–189 (2004).
33. M. Sakowicz-Burkiewicz, G. Nishanth, U. Helmuth, K. Drögemüller, D. H. Busch, O. Utermöhlen, M. Naumann, M. Deckert, D. Schlüter, Protein kinase C-θ critically regulates the proliferation and survival of pathogen-specific T cells in murine listeriosis. *J. Immunol.* **180**, 5601–5612 (2008).
34. N. N. Berg-Brown, M. A. Gronski, R. G. Jones, A. R. Elford, E. K. Deenick, B. Odermatt, D. R. Littman, P. S. Ohashi, PKCθ signals activation versus tolerance in vivo. *J. Exp. Med.* **199**, 743–752 (2004).
35. B. J. Marsland, C. Nembrini, N. Schmitz, B. Abel, S. Krautwald, M. F. Bachmann, M. Kopf, Innate signals compensate for the absence of PKC-θ during in vivo CD8$^+$ T cell effector and memory responses. *Proc. Natl. Acad. Sci. U.S.A.* **102**, 14374–14379 (2005).
36. G. Fu, O. L. Wijburg, P. U. Cameron, J. D. Price, R. A. Strugnell, *Salmonella enterica* serovar Typhimurium infection of dendritic cells leads to functionally increased expression of the macrophage-derived chemokine. *Infect. Immun.* **73**, 1714–1722 (2005).
37. G. Fu, S. Vallée, V. Rybakin, M. V. McGuire, J. Ampudia, C. Brockmeyer, M. Salek, P. R. Fallen, J. A. H. Hoerter, A. Munshi, Y. H. Huang, J. Hu, H. S. Fox, K. Sauer, O. Acuto, N. R. J. Gascoigne, Themis controls thymocyte selection through regulation of T cell antigen receptor–mediated signaling. *Nat. Immunol.* **10**, 848–856 (2009).
38. G. Fu, N. R. J. Gascoigne, Multiplexed labeling of samples with cell tracking dyes facilitates rapid and accurate internally controlled calcium flux measurement by flow cytometry. *J. Immunol. Methods* **350**, 194–199 (2009).
39. C. Krieg, O. Boyman, Y. X. Fu, J. Kaye, B and T lymphocyte attenuator regulates CD8$^+$ T cell–intrinsic homeostasis and memory cell generation. *Nat. Immunol.* **8**, 162–171 (2007).
40. M. B. Lutz, N. Kukutsch, A. L. Ogilvie, S. Rossner, F. Koch, N. Romani, G. Schuler, An advanced culture method for generating large quantities of highly pure dendritic cells from mouse bone marrow. *J. Immunol. Methods* **223**, 77–92 (1999).
41. R. E. Campbell, O. Tour, A. E. Palmer, P. A. Steinbach, G. S. Baird, D. A. Zacharias, R. Y. Tsien, A monomeric red fluorescent protein. *Proc. Natl. Acad. Sci. U.S.A.* **99**, 7877–7882 (2002).

Acknowledgments: We thank A. Altman (La Jolla Institute for Allergy and Immunology), K. Hogquist and S. Jameson (University of Minnesota, Minneapolis), and D. Littman (Skirball Institute, New York) for mice and reagents, and the TSRI Mouse Genetics Core for help in making the knockout mice. **Funding:** This work was supported by grants from NIH (GM048002 and GM065230 to N.R.J.G., OD006433 to H.C., and AI070845 to K.S.). N.N.-M. was supported by a fellowship from the Swiss National Science Foundation; J.C. was supported by a fellowship from the Spanish Ministerio de Ciencia e Innovacion; P.P.Y. was supported by NIH training grant T32HL07195; J.A.H.H. was supported by the Irving S. Sigal Fellowship of the American Chemical Society and by NIH training grant T32AI07244; and K.S. was supported by The Leukemia & Lymphoma Society Scholar Award 1440-11. The content of this work is solely the responsibility of the authors and does not necessarily represent the official views of the National Institute of General Medicine or the NIH. This is manuscript number 20858 from The Scripps Research Institute. **Author contributions:** G.F. and N.R.J.G. designed the project; G.F. made the knockout mice with help from B.M.; G.F., J.H., A.L.G., F.L., S.F., H.C., J.A.H.H., and J.A. analyzed the mice; V.R., S.R., and K.S. performed or analyzed biochemical experiments; G.F., J.C., P.P.Y., and N.N.-M. performed imaging; N.N.-M. made the initial finding that PKCη abundance was increased during thymocyte development; and G.F. and N.R.J.G. wrote the manuscript. **Competing interests:** The authors declare that they have no competing interests.

Submitted 31 March 2011
Accepted 16 November 2011
Final Publication 6 December 2011
10.1126/scisignal.2002058
Citation: G. Fu, J. Hu, N. Niederberger-Magnenat, V. Rybakin, J. Casas, P. P. Yachi, S. Feldstein, B. Ma, J. A. H. Hoerter, J. Ampudia, S. Rigaud, F. Lambolez, A. L. Gavin, K. Sauer, H. Cheroutre, N. R. J. Gascoigne, Protein kinase C η is required for T cell activation and homeostatic proliferation. *Sci. Signal.* **4**, ra84 (2011).

Downloaded from stke.sciencemag.org on December 15, 2011